Facet-Selective Epitaxial Growth of Heterogeneous Nanostructures of Semiconductor and Metal: ZnO Nanorods on Ag Nanocrystals

Feng-Ru Fan,[†,‡] Yong Ding,[†] De-Yu Liu,[‡] Zhong-Qun Tian,*,[‡] and Zhong Lin Wang*,[†]

School of Materials Science and Engineering, Georgia Institute of Technology, Atlanta, Georgia 30332-0245, and State Key Laboratory of Physical Chemistry of Solid Surfaces, Department of Chemistry, College of Chemistry and Chemical Engineering, Xiamen University, Xiamen 361005, China

An important frontier in nanomaterials synthesis is the growth of crystalline overlayers on different nanostructures with controlled chemical and physical properties and new functionalities.[1] Metal−semiconductor heterogeneous nanostructures have attracted great attention because of their unique optical, electrical, and catalytic properties and potential applications in developing future optoelectronic devices in nanosystems.[2] Many multifunctional metal−semiconductor nanostructures have been prepared to date by wet chemical routes, including core−shell structures such as Au@PbS, Au@CdS, Au@Ag$_2$S, and Au@ZnS,[3] as well as by loading metal tips or dots onto semiconductors, yielding materials such as Au−CdS, Au−CdSe, Pt−CdS, and Au or Ag on ZnO.[4,5]

Anisotropy is a fundamental nature of crystal structure. The various facets in a crystal may exhibit different physical and chemical properties that are deeply direction-dependent. Nanoparticles of Ag, one of the typical fcc noble metals, are usually enclosed by low-index {111} and {100} surfaces.[6] A key difference between {111} and {100} facets is the atomic arrangement and lattice symmetry and spacing. Ingeniously, this fact has been applied to upgrade shape-dependent reaction selectivity in catalysis.[7] Similarly, it should also allow the selective growth of one nanomaterial on a specific crystal surface of the other material to afford novel heterogeneous nanostructures through reasonable design and control of the growth environment. Here we demonstrate the application of structure specificity in a colloidal synthesis system by introducing a method that spontaneously achieves facet-selective growth of ZnO nanorods on {111} rather than {100} facets of Ag nanocrystals. By relying on systematic characterization, we have identified the fine structures and explained the formation mechanism of these nanostructures.

Ag−ZnO heterogeneous nanostructures were prepared by a seed-mediated method. The ZnO nanorods were overgrown on the specific surface of Ag truncated nanocubes (Figure S1) in aqueous solution[8] (see the Supporting Information for details). Figure 1 shows representative scanning electron microscopy (SEM) images of Ag−ZnO heterogeneous nanostructures with different numbers of nanorods grown on single Ag seeds obtained in a one-pot procedure. The low-magnification SEM image shows that a majority of the prepared structures adopt a combination of a Ag seed and ZnO nanorods (Figure S2). ZnO nanorods can grow directly on the facets of Ag without any other ancillary seed-assisted process. A maximum of seven nanorods can be observed on a single Ag nanocrystal as a result of the confined space; this was also confirmed by transmission electron microscopy (TEM) (Figure S3). This phenomenon implies that ZnO nanorods may selectively grow on the eight {111} rather than the six {100} facets of a Ag nanocrystal.
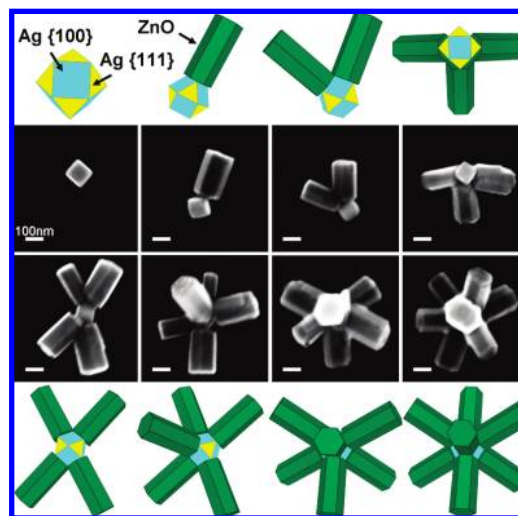

Figure 1. SEM images showing the selective growth of different numbers of ZnO nanorods on the {111} facets of Ag truncated nanocubes. The corresponding geometrical models of the heterogeneous nanostructures are presented. The yellow and cyan planes represent the {111} and {100} facets of Ag, respectively; the green planes represent the facets of the ZnO nanorods.

The crystal structures of the as-prepared nanocrystals were characterized by X-ray diffraction (XRD) and energy-dispersive X-ray spectroscopy (EDS) (Figure S4), which showed that there are two separate phases, fcc Ag and wurtzite ZnO. The head and tails of the heterogeneous nanostructures are composed of a pure Ag nanoparticle and ZnO nanorods, respectively.

To confirm our hypothesis of preferential growth of ZnO nanorods on Ag nanocrystals and obtain deeper insight into the nature of the heterogeneous nanostructures, we performed characterizations using selected-area electron diffraction (SAED) and convergent-beam electron diffraction (CBED) measurements. Figure 2a,b shows TEM images of single Ag nanoparticles connected with one and two ZnO nanorods, respectively. All of the ED spots (Figure 2a,b insets) taken from each Ag nanoparticle and ZnO nanorod are aligned as two-dimensional arrays, showing that both of them are single-crystalline structures. The patterns recorded from the ZnO nanorods were along the [01$\bar{1}$0] zone axis and those of Ag nanoparticles along [$\bar{1}$12], indicating that the epitaxial relationships are [01$\bar{1}$0]$_{ZnO}$ ∥ [$\bar{1}$12]$_{Ag}$ and (0002)$_{ZnO}$ ∥ (111)$_{Ag}$. It is clear that the growth direction of the ZnO nanorods coincides with the <111> direction of the Ag nanocrystal. Therefore, the ZnO nanorods directly grow on the {111} facets of Ag nanocrystals along their own *c*-axis direction. As a supplementary proof of this point, analysis of the angles between two ZnO nanorods gave 67.5 and 111°, in good agreement with the calculated angles of two adjacent

† Georgia Institute of Technology.
‡ Xiamen University.
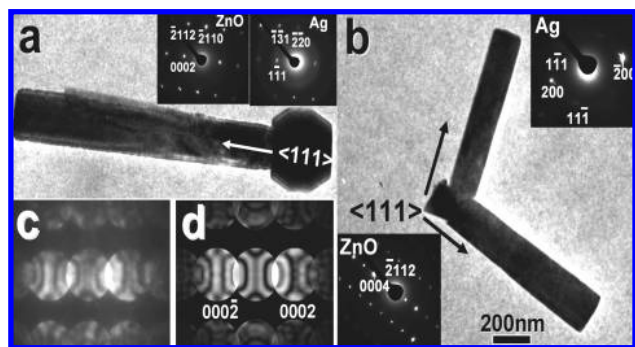
Figure 2. TEM images of the growth of (a) one and (b) two ZnO nanorods on a single Ag truncated nanocube. The insets are the corresponding SAED patterns taken from the Ag nanoparticles and ZnO nanorods. The arrows indicate that the growth direction of ZnO is along the <111> zone axis of the Ag seeds. (c) Experimental and (d) simulated CBED patterns of the ZnO nanorod in (a) for determining the atomic layer directly facing the Ag particle.

{111} planes, 70.5 and 109.5° along the projection directions, respectively (Figure S5).

The polar direction of the ZnO nanorod was identified by CBED. A comparison of the experimental CBED pattern with a theoretically calculated pattern is given in Figure 2c,d. The intensity distributions in the (0002) and the (000$\bar{2}$) disks exhibit excellent agreement,[9] indicating that the end of the ZnO nanorod directly interfacing with the Ag nanoparticle is along [0001], which in turn indicates that Zn atoms are the first layer bonded to the surface of Ag seeds and that the growth front of the nanorod is an oxygen layer.

Lattice mismatch is known to play a significant role in the epitaxial growth of heterogeneous structures via gas-phase deposition, electrical deposition, and solution-phase conformal epitaxial growth.[10] A high degree of lattice mismatch prevents the nucleation and growth of an overlayer on a substrate because of the high structural strain. In this study, the {111} facet of Ag has hexagonal symmetry, the same as the basal {0001} facet of hexagonal ZnO (Figure 3a). From the SAED data in Figure 2a, the Ag($\bar{1}$12) plane (lattice-plane spacing $d = 0.16697$ nm) matches the ZnO ($2\bar{1}\bar{1}0$) plane ($d = 0.1625$ nm), with a mismatch of only 2.68%. In comparison, the {100} facet adopts square close-packed arrangement, leading to the formation of a large structure mismatch (Figure 3b). Additionally, the lattice mismatch between ZnO and Ag(100) is as high as 23.9%. Therefore, the {111} facet with a better structure match is more favorable for the nucleation and growth of ZnO. We believe that the nature of the facet-selective growth is caused by the structural match. It should be noted that the growth of the overlayer could be influenced considerably by the reaction temperature, the concentration of reducing agent, and the surfactant. For instance, it has been observed that poly(vinyl pyrrolidone), a surfactant commonly used in the synthesis of Ag nanostructures, tends to preferentially cover the {100} facets rather than the {111} facets.[11]

In summary, we have demonstrated for the first time that ZnO nanorods preferentially grow on the {111} rather than the {100} facets of truncated Ag nanocubes in aqueous solution. The growth mechanism is attributed to two factors. The first factor is a good lattice and symmetry match between ZnO and Ag in the corresponding planes. The other is the direct interfacing of the Zn layer
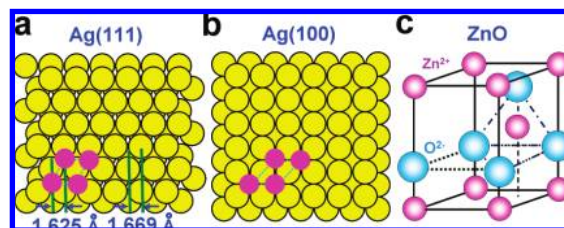
Figure 3. Representation of the structure mismatch between the ZnO lattice and Ag surfaces with different crystal planes. (a, b) Hexagonal structure units of oxygen atoms arranged on (a) {111} and (b) {100} facets of fcc Ag. (c) Schematic model of ZnO with the wurtzite structure.

with Ag that initiates the formation of the ZnO lattice. The approach and mechanism proposed here could be applicable to other possible combinations of metal−semiconductor heterojunctions. The heterogeneous nanostructures are of special interest for studying electrical contacts, functional devices, biological sensors, and catalysis using metal−semiconductor heterostructures.

Supporting Information Available: Experimental details and additional data. This material is available free of charge via the Internet at http://pubs.acs.org.

References

(1) Cozzoli, P. D.; Pellegrino, T.; Manna, L. *Chem. Soc. Rev.* **2006**, *35*, 1195.
(2) (a) Enache, D. I.; Edwards, J. K.; Landon, P.; Solsona-Espriu, B.; Carley, A. F.; Herzing, A. A.; Watanabe, M.; Kiely, C. J.; Knight, D. W.; Hutchings, G. J. *Science* **2006**, *311*, 362. (b) Lee, J. S.; Shevchenko, E. V.; Talapin, D. V. *J. Am. Chem. Soc.* **2008**, *130*, 9673. (c) Zhang, W. Q.; Lu, Y.; Zhang, T. K.; Xu, W.; Zhang, M.; Yu, S. H. *J. Phys. Chem. C* **2008**, *112*, 19872.
(3) (a) Shi, W. L.; Zeng, H.; Sahoo, Y.; Ohulchanskyy, T. Y.; Ding, Y.; Wang, Z. L.; Swihart, M.; Prasad, P. N. *Nano Lett.* **2006**, *6*, 875. (b) Chen, W. T.; Yang, T. T.; Hsu, Y. J. *Chem. Mater.* **2008**, *20*, 7204. (c) Liu, M. Z.; Guyot-Sionnest, P. *J. Mater. Chem.* **2006**, *16*, 3942. (d) Sun, Z. H.; Yang, Z.; Zhou, J. H.; Yeung, M. H.; Ni, W. H.; Wu, H. K.; Wang, J. F. *Angew. Chem., Int. Ed.* **2009**, *48*, 2881.
(4) (a) Mokari, T.; Rothenberg, E.; Popov, I.; Costi, R.; Banin, U. *Science* **2004**, *304*, 1787. (b) Mokari, T.; Sztrum, C. G.; Salant, A.; Rabani, E.; Banin, U. *Nat. Mater.* **2005**, *4*, 855. (c) Habas, S. E.; Yang, P. D.; Mokari, T. *J. Am. Chem. Soc.* **2008**, *130*, 3294. (d) Subramanian, V.; Wolf, E. E.; Kamat, P. V. *J. Phys. Chem. B* **2003**, *107*, 7479. (e) Pacholski, C.; Kornowski, A.; Weller, H. *Angew. Chem., Int. Ed.* **2004**, *43*, 4774.
(5) (a) Zheng, Y. H.; Zheng, L. R.; Zhan, Y. Y.; Lin, X. Y.; Zheng, Q.; Wei, K. M. *Inorg. Chem.* **2007**, *46*, 6980. (b) Yao, T.; Yan, W. S.; Sun, Z. H.; Pan, Z. Y.; He, B.; Jiang, Y.; Wei, H.; Nomura, M.; Xie, Y.; Xie, Y. N.; Hu, T. D.; Wei, S. Q. *J. Phys. Chem. C* **2009**, *113*, 3581.
(6) (a) Wang, Z. L. *J. Phys. Chem. B* **2000**, *104*, 1153. (b) Wiley, B.; Sun, Y. G.; Mayers, B.; Xia, Y. N. *Chem.—Eur. J.* **2005**, *11*, 454.
(7) (a) Chen, M. S.; Kumar, D.; Yi, C. W.; Goodman, D. W. *Science* **2005**, *310*, 291. (b) Bratlie, K. M.; Lee, H.; Komvopoulos, K.; Yang, P. D.; Somorjai, G. A. *Nano Lett.* **2007**, *7*, 3097. (c) Christopher, P.; Linic, S. *J. Am. Chem. Soc.* **2008**, *130*, 11264.
(8) (a) Sun, Y. G.; Xia, Y. N. *Science* **2002**, *298*, 2176. (b) Vayssieres, L. *Adv. Mater.* **2003**, *15*, 464.
(9) (a) Wang, Z. L.; Kong, X. Y.; Zuo, J. M. *Phys. Rev. Lett.* **2003**, *91*, 185502. (b) Zhou, X.; Xie, Z. X.; Jiang, Z. Y.; Kuang, Q.; Zhang, S. H.; Xu, T.; Huang, R. B.; Zheng, L. S. *Chem. Commun.* **2005**, 5572.
(10) (a) Golan, Y.; Hodes, G.; Rubinstein, I. *J. Phys. Chem.* **1996**, *100*, 2220. (b) Habas, S. E.; Lee, H.; Radmilovic, V.; Somorjai, G. A.; Yang, P. *Nat. Mater.* **2007**, *6*, 692. (c) Fan, F. R.; Liu, D. Y.; Wu, Y. F.; Duan, S.; Xie, Z. X.; Jiang, Z. Y.; Tian, Z. Q. *J. Am. Chem. Soc.* **2008**, *130*, 6949.
(11) Sun, Y. G.; Mayers, B.; Herricks, T.; Xia, Y. N. *Nano Lett.* **2003**, *3*, 955.

JA9036324